Electroless Nickel Plating on Magnesium Alloy

P-05124

by A.K. Sharma, M.R. Suresh, H. Bhojraj, H. Narayanamurthy, and R.P. Sahu,
ISRO Satellite Centre, Bangalore, India

The inherent lightness and good strength-to-weight ratio of magnesium has focused attention on increasing applications in aerospace and allied fields. Its density is two thirds that of aluminum—a conventional structure material for aerospace. Magnesium has one drawback: It is prone to atmospheric corrosion. Further, because of its high chemical affinity for aqueous solutions, it is categorized as a difficult metal for electrochemical treatments. The highly reactive nature of magnesium is clearly indicative by its position in the electromotive series ($E° = -2.37$ V). The situation is still more complex for magnesium alloys, where the alloying constituents introduce electrochemical heterogeneity.[1,2]

Communication satellites make use of a traveling wave tube (TWT) for amplification of signals. In a TWT the collector is the main source of heat dissipation. The electrodes are heated by the residual kinetic energy of the collected electrons; however, the electrodes must be maintained at a relatively low temperature. There are two ways to dissipate this heat into cold space (see Fig. 1).

1. Heat conduction from the electrodes to the spacecraft radiator. This is called conduction cooling and is suit-able only for low- and medium-power tubes.

2. Heat radiation or conduction from the electrodes to a radiator, which is an integral part of TWT. This is called radiation cooling and is suitable for even high-power TWTs.

The latter cooling method simplifies spacecraft thermal control. A fin structure is attached to the collector end to increase the heat transfer area, and a high-emittance coating is applied over it to improve heat-radiation characteristics. A total assembly of high-power TWT employing radiative cooling is shown in Figure 2.

The radiator, top collector, and base plates of TWT shown in Figures 3 to 5 were made out of magnesium alloy ZM21. In a conventional TWT, these are, however, fabricated out of aluminum alloys. The magnesium alloy ZM21 was selected because of its inherent lightness and higher thermal conductance over conventional magnesium alloys. The radiator requires a high-emittance coating on the exposed portion to reject the heat in space. The inner area of the radiator and the complete surface of the top collector and base plates are to be coated with a high-corrosion-resistance coating with good solderability characteristics. These coatings should withstand elevated temperature for an extended period without degradation in their properties.

In an earlier communication,[3] a process for anodization on magnesium alloy ZM21 that provides a high-emittance coating (0.90) over a wide temperature range was described. In the present article, an electroless nickel process is described. The process provides a high degree of corrosion resistance at elevated temperatures and a good solderability and wettability to the soldering material.

Electroless nickel-phosphorus coatings are generally favored over electroplated deposits because of their enhanced corrosion-resistance properties and the coating uniformity achievable with complex objects. Each system has its advantages and disadvantages, but the properties of electroless nickel and its ability to incorporate composites have enabled the process to be ex-
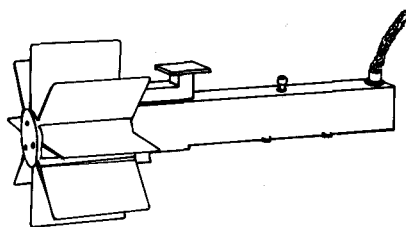

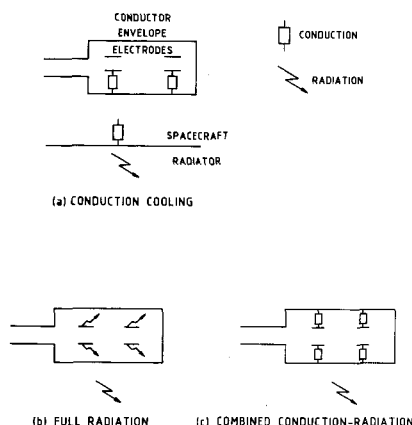Figure 2. High-power traveling wave tube.

(a) CONDUCTION COOLING

(b) FULL RADIATION   (c) COMBINED CONDUCTION-RADIATION

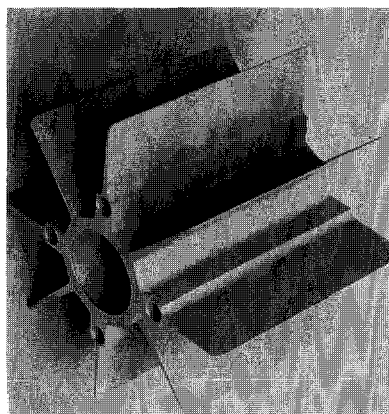Figure 1. Collector conduction and radiation cooling principle.
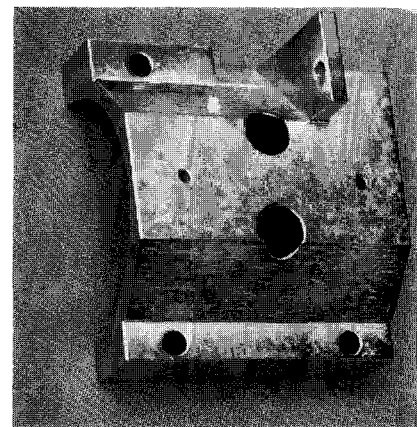
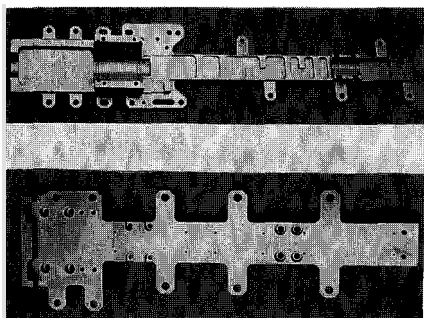

Figure 3. Radiator.

Figure 4. Top collector.

Figure 5. Base plates.

ploited widely. The advantages of the electroless coatings[4] include:

- Good throwing power
- Uniform coating thickness on complex objects
- No leveling required
- Coatings are harder (480 HV) than electrodeposited metal (200 HV) because phosphorus is incorporated in the structure
- Deposits can be further hardened to about 1,050 HV by heat treatment at about 400°C for 1 hr
- Good wear resistance
- Low ductility (1-3% elongation)
- Low porosity, which leads to good corrosion resistance
- Excellent solderability and brazability characteristics
- Low labor cost

The main disadvantages of electroless system are:

- Solutions are expensive
- Deposition rates are slow
- Welding characteristics are poor
- Careful analytical control of the bath is required

Electroless nickel is an engineering coating primarily used for its unusual combination of corrosion and wear-resistance properties. It differs significantly from electroplated nickel as it is an alloy of nickel and phosphorus. The coating properties can be tailored by optimizing the alloy composition, that is, variation in the phosphorus content in the range of 5 to 12%. The phosphorus content of the deposit depends mainly on the pH control of the bath during plating, but it is also affected by its formulation (complexing and buffering agents), the plating bath temperature, and the molar ratio of nickel to hypophosphite.[5] As the phosphite con-

centration increases during the life of the bath, the phosphorus content of the deposit gradually increases.

Other differences in deposit properties are frequent because of variation in heat treatment temperature and time after plating. As plated, electroless nickel is in a metastable state consisting of a supersaturated solid solution of phosphorus in nickel, because the equilibrium solid solubility of phosphorus in nickel is essentially zero; however, the second phase cannot form because the time interval between the deposition of successive layers is too short for the necessary diffusion. The structure of the deposit changes from microcrystalline to amorphous with increasing alloy content. The second phase, which is Ni_3P, can form on annealing and results in precipitation hardening.[6]

When electroless nickel deposits are heated above 220°C, they begin to crystallize, and nickel phosphide precipitates from supersaturated nickel phosphide solid solutions. These nickel phosphides are found in many forms and have been identified by X-ray diffraction to include Ni_3P alloy with several other structures. The primary effects of crystallization and nickel phosphide precipitation are hardening and shrinkage of the coating alloy (leads to microcracking), with reduced ductility and corrosion resistance. These changes also produce a more wear-resistant surface.

The maximum hardness in electroless nickel deposits can be attained in 1 hr at about 400°C or 10 hr at 260°C. The ability of deposits to maintain their hardness under elevated temperature service conditions increases with increasing phosphorus content but decreases rapidly above 385°C.

Electroless nickel is most frequently used in wear applications in the precipitation-hardened condition because of improved hardness and natural lubricity. The corrosion resistance deteriorates upon heat treatment above 250°C because of cracking; therefore, under corrosive wear applications, it may be prudent to forgo the higher hardness. Electroless nickel is also applied to improve solderability and brazability of surfaces and is used with molds and dies to improve lubricity and part release.

Table I. Chemical Composition and Properties of Magnesium Alloy ZM21

Properties	Value
Chemical composition (% by weight)	Zn 2.03; Mn 0.81; Fe 0.03; Si 0.29; Mg balance
Density (g/cm²)	1.8
Ultimate tensile strength (kg/mm²)	
20°C	24.0
200°C	11.7
Yield strength (0.2% proof strength MPa) (kg/mm²)	
20°C	12.0
200°C	8.3
Thermal conductivity (W/m K)	
20°C	114
100°C	120
200°C	129
% Elongation	21–25

EXPERIMENTAL DETAILS

The studies were performed on the samples of magnesium alloy ZM21. The chemical composition and properties of the alloy are presented in Table I. This alloy was selected because it provides higher thermal conductance than other conventional magnesium alloys. Because the plating requirements are crucial inside the deep narrow holes, experiments were conducted on the specimens specially designed for this work, as shown in Figure 6. The vent holes were provided for better coverage of the coating inside the functional holes. Table II gives the sequence of operations performed.

Heat treatment after electroless nickel deposition results in an atomic diffusion between basis metal and coating material. The coating becomes more adherent because of the formation of a diffusion alloying interface.[7] Because the present coatings are proposed to be used for nonwear-resis-
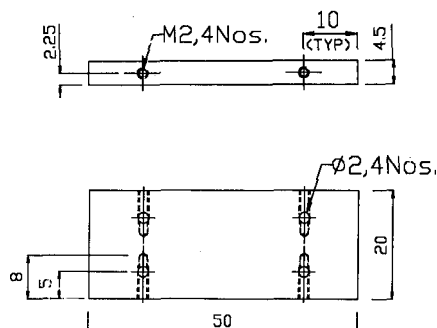

Figure 6. Specimens for electroless nickel plating (all dimensions are in mm).

Table II. Sequence of Operations

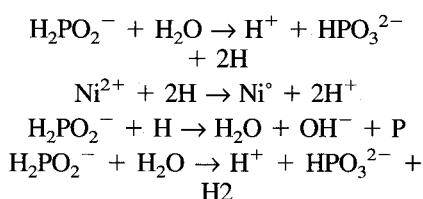| Stage No.	Process Operation	Condition
1.	Ultrasonic degreasing	Isopropanol for 5–10 min
2.	Alkaline cleaning	
	Sodium hydroxide, NaOH	50 g/L
	Trisodium orthophosphate, $Na_3PO_4 \cdot 12H_2O$	10 g/L
	Temperature	60 ± 5°C
	Time	8–10 min
3.	Water rinse	
4.	Acid pickling	
	Chromium trioxide, CrO_3	125 g/L
	Nitric acid (70% V/V)	110 ml/L
	Temperature	Room temperature (20°C)
	Agitation	Vigorous, mechanical
	Time	45–60 sec
5.	Water rinse	
6.	Fluoride activation	
	Hydrofluoric acid, HF (40%V/V)	385 ml/L
	Temperature	Room temperature (20°C)
	Agitation	Mild, mechanical
	Time	10 min
7.	Water rinse	
8.	Electroless nickel plating	
	Basic nickel carbonate	10 g/L
	$NiCO_3 \cdot 2Ni(OH)_2 \cdot 4H_2O$	
	Hydrofluoric acid, HF (40% V/V)	12 ml/L
	Citric acid, $C_6H_8O_7 \cdot H_2O$	5 g/L
	Ammonium bifluoride, NH_4H_2	10 g/L
	Ammonia solution (25% V/V)	30 ml/L
	Sodium hypophosphite	20 g/L
	Thiourea	1 mg/L
	pH	6.5±1.0
	Temperature	80 ± 2°C
	Job agitation	Mild, mechanical continuous
	Solution filtration	Continuous
	Time	60 min
9.	Water rinse	
10.	Passivation treatment to improve the corrosion resistance of electroless nickel coating. The treatment was carried out by immersion of work in a solution containing chromium trioxide 2.5 g/L and sodium dichromate 120 g/L, operating at 90 to 100°C for 10 to 15 min.	
11.	Hot water dip and air dry	
12.	Heat treatment at 230°C for 2 hr. The heat treatment was carried out in an oven with filtered hot air circulation facility for dust-free and uniform temperature distribution.	

Figure 7. Variation in coating thickness with time (pH 6.5, 80°C).

tance applications, heat treatment was restricted to 230°C. Heat treatment beyond 250°C increases the microhardness of the coating because of microcrack hardening but reduces their corrosion-resistance value.
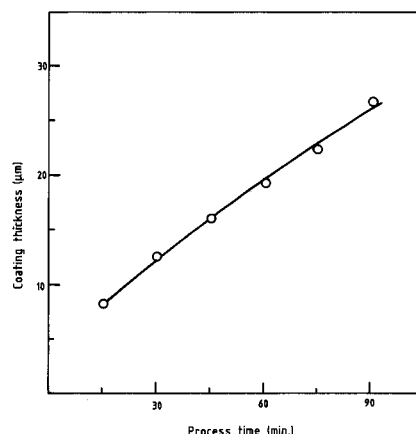
RESULTS AND DISCUSSION

In the present formulation the function of basic nickel carbonate is to provide nickel ions, and the sodium hypophosphite acts as a metal-reducing agent. The plating solution also contains citric acid and bifluoride, which act as buffers, complexing agents, and accelerators. Thiourea acts as a solution stabilizer and brightening agent, and ammonia solution is used to adjust the pH of the plating solution.

The autocatalytic reaction for nickel deposition is initiated by catalytic dehydrogenation of the reducing agent with release of hydride ion, which then supplies electrons for the reduction of nickel ions.

$$H_2PO_2^- + H_2O \rightarrow H^+ + HPO_3^{2-} + 2H$$
$$Ni^{2+} + 2H \rightarrow Ni^\circ + 2H^+$$
$$H_2PO_2^- + H \rightarrow H_2O + OH^- + P$$
$$H_2PO_2^- + H_2O \rightarrow H^+ + HPO_3^{2-} + H2$$

In reality there will always be less nickel and more hydrogen produced than indicated earlier here. The nickel deposits in general were found to contain 3 to 15% codeposited phosphorus originating from hypophosphite ion. The phosphorus content results in deposit properties different from those of electrodeposited nickel and accounts for some of the applications of electroless nickel.

BATH OPTIMIZATION

Bath optimization of electroless nickel was based on the assessment of deposition rate and surface topography, the variables being plating time, bath temperature, and pH.

Figure 7 shows the variation of coating thickness with plating time at a constant electrolyte temperature and pH. The film growth is directly related to the plating time. A slight decrease in deposition rate with time was observed, which may be attributed to the reduction of reactants in the electrolyte. The results were found to be reproducible within ± 3%.

The effect of bath temperature on deposition rate is shown in Figure 8. This shows the expected rapid increase in the deposition with rise in bath temperature. The coating deposition was almost nil at bath temperatures below 50°C. When the bath was operated above 80°C, the deposition rate was too high. The coatings appeared powdery, and a drop in microhardness value was observed. The optimum results were obtained with electrolyte operating temperature at 80 ± 2°C.

Figure 9 shows the dependence of deposition rate on bath pH. At pH 4.0 and below, heavy dissolution of sub-
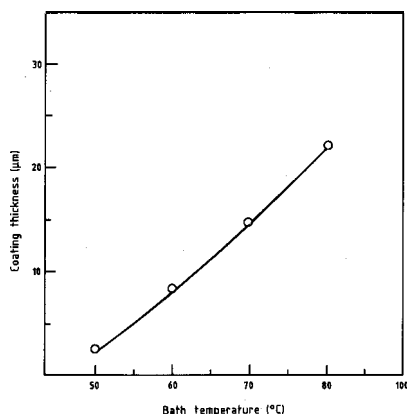
Figure 8. Influence of bath temperature on coating growth (pH 6.5, 60 min).

strate was observed. The deposits were powdery, with little or no adherence. At pH > 8.0, the deposits were stressed. This was noticed when the coating was cut. This may be attributed to low phosphorus content.

As the high tensile stress has a detrimental effect on the corrosion resistance of the deposit, it is desirable to obtain a deposit with low tensile stress. The optimum coating deposition was obtained at pH 6.5 ± 1.0.

STUDIES ON DIMENSIONAL CHANGE

The dimensional change associated with various steps of electroless nickel plating was investigated. The studies were performed by accurate measurements of both the dimensions and weight of specimens before and after each preplating step.

The percentage difference in the values obtained by both the methods was within ± 1.5%. For each set of exper-
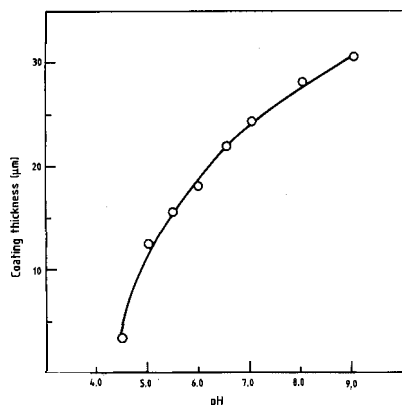

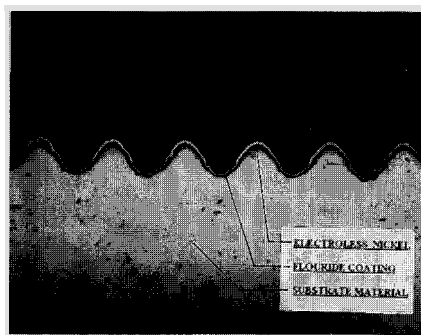**Figure 9. Influence of electrolyte pH on coating growth (80°C, 60 min).**

iments measurements were made on seven fine-machined coupons, and the average value was obtained. The data of change in dimension due to different preplating steps are: alkaline cleaning, negligible (not measurable); acid pickling, 1 μm/sec; fluoride activation, 0.08 μm/min.

MECHANICAL PROPERTIES

Adhesion of electroless nickel specimens was evaluated by a heat-quench test. The specimens were heated at 250°C for 2 hr and quenched in air. No discoloration, cracks, blisters, or peeling of the coating was observed. The adhesion test was repeated on the test specimens after humidity, thermal cycling, and thermovacuum performance tests.

The thickness of electroless nickel coating was measured on the surface and inside the holes by microsectioning. The test specimens were carefully cut using a diamond cutter. The cut test samples were mounted using Epo-Kwick resin and Epo-Kwick hardness (Buehler Ltd., USA) in a 5:1 ratio, cured for 6 hr at room temperature, and then metallographically polished. The thickness of electroless nickel was then measured on a graduated scale optical microscope (500×). The average thickness of electroless nickel was 22.4 μm on the surface and 13.1 μm inside the bottom of the holes. A photomicrograph of a representative specimen, showing the coating thickness, is given in Figure 10.

The microhardness of electroless nickel was measured using a diamond indentor. Vickers hardness numbers were obtained by averaging seven measurements of each specimen with a load of 50 g. The microhardness of electroless nickel before heat treatment

Figure 10. Photomicrograph of a representative specimen showing coating thickness inside holes.

was in the range of 760 to 785 VHN. An increase in Vickers hardness number by 55 to 65 was observed after heat treatment at 230°C for 2 hr.

The change in hardness with heat treatment is associated with structural transformation, precipitation, and/or agglomeration of nickel phosphide (Ni_3P) particles. The microstructure of the electroless nickel sample as plated was indicative of a fine dispersion of a thin layer of precipitated phosphorus in nickel, whereas the structure of the coating after heat treatment at or above 230°C showed dispersion of nickel in a matrix of nickel phosphide.

The density of electroless nickel was determined by the accurate measurement of associated dimensional change. Electroless nickel of approximately 25 μm thick was deposited on one side of a thin, flat magnesium specimen (the other side was masked by a stop-off lacquer). The mass and dimensions of the test coupon were accurately measured with a three-coordinate measuring machine (least count 1 μm). The coating thicknesses were determined under a graduated-scale microscope after metallographic polishing. The difference in both the measurements was within ± 1 μm. The density of electroless nickel coatings was found in the range of 7.28 to 7.32 g/cm^3.

ENVIRONMENTAL STABILITY

To evaluate the environmental stability of the coatings for ground and space applications, the plated test coupons were subjected to humidity, corrosion resistance, thermal stability, thermal cycling, and thermovacuum performance tests.

Humidity Test

The humidity test was carried out to examine the effect of high humidity and temperature, which in turn shows the resistance of the coating to the corrosive prelaunch environment. The test was conducted in a thermostatically controlled humidity chamber for 48 hr. Relative humidity of 95 ± 0.5% was maintained in the chamber at 50 ± 1°C. The test specimens were then examined visually, and their optical properties were measured. No sign of any physical degradation or change in optical properties was observed.

Corrosion-Resistance Test

To evaluate the resistance of electroless nickel coating against the corrosive ground atmosphere, an accelerated corrosion test was conducted. The test coupons were immersed in a 5% solution of sodium chloride at pH 7.0, and the time taken for discoloration of the coating or formation of corrosion spots was carefully observed. The test indicated adequate stability because no discoloration or corrosion spots in the coating were noticed after 96 hr of immersion. The formation of corrosion spots initiated only after the fifth day of immersion.

Thermal Stability Test

The electroless nickel coating is required in some of the high-heat dissipating parts where the temperature may exceed 200°C for an extended period. The thermal stability test consists of heating five electroless nickel-plated coupons in a vacuum oven for 48 hr. The temperature of the oven was maintained at $250 \pm 2°C$ and a vacuum level of 10^{-5} torr throughout the experiment. The specimens were then examined visually for any degradation. No physical degradation of any kind was noticed.

Thermal Cycling Test

A satellite in orbit experiences extreme temperatures. It experiences low temperature when it dives into the earth's shadow and becomes extremely hot when exposed to direct sunlight. The thermal cycling test is designed to evaluate the effect of cycling temperatures on the coating that are likely to be encountered throughout the life span of a spacecraft. The test was conducted in a thermostatically controlled hot-and-cold chamber. A cycle consists of placing the test coupons into a cold chamber for a dwell of 5 min, bringing the test coupons to an ambient temperature with a dwell of 15 min, and shifting the coupons to a hot chamber with a dwell of 5 min. One hundred cycles of each of the following extreme temperatures were applied: −50°C/100°C; 0°C/150°C; and 50°C/200°C.

After thermal cycling the specimens were inspected visually. No degradation of any kind was observed on the surface of test specimens.

Thermovacuum Performance Test

This test is designed to examine the effect of temperature on the coatings in vacuum (space environment). The test was carried out in a thermostatically controlled thermovacuum chamber. The test consists of maintaining the test chamber at lower temperature for 2 hr and then raising the temperature to higher temperature and maintaining it for 2 hr (thermovacuum cold-and-hot soak test). A total of 10 cycles of cold-and-hot soak were applied. A vacuum level of 10^{-5} torr was maintained inside the test chamber during the entire test period. The extreme temperature limits for thermovacuum test were same as used for thermal cycling test.

SOLDERABILITY TEST

Electroless nickel-phosphorus alloys are easily soldered with a highly active acid flux. Soldering without a flux, or with mildly active fluxes, is more difficult if the parts are allowed to form oxides by any extended exposure to atmosphere. Heat treatment of electroless nickel-plated parts can make soldering extremely difficult unless a highly active acid flux is used.

The present solderability test is designed to evaluate the solderability as well as wettability of soldering material to the electroless nickel coating. The test comprises soldering of plated samples and evaluation of solder joints by pull test for mechanical characterization of solder joint interface.

Preparation of Test Sample

The test sample is made of two pieces, as shown in Figure 11a and b. These pieces were electroless nickel plated to about 20 μm coating thickness. The two pieces were matched, as shown in Figure 11c, and placed on an aluminum jig. To fill the gap x of 0.2 mm with solder, the jig along with sample pieces was heated on a hot plate to the melting temperature of solder (350–400°C). Organic activated Rosin Flux No. 1429 (Kester, USA) and Sn 63 Pb 37 solder (Multicore, UK) were used. The sample pieces were slowly moved by actuating the screws of the jig until the gap was completely filled.

After cooling, the solder assembly was machined, as shown in Figure 11d.
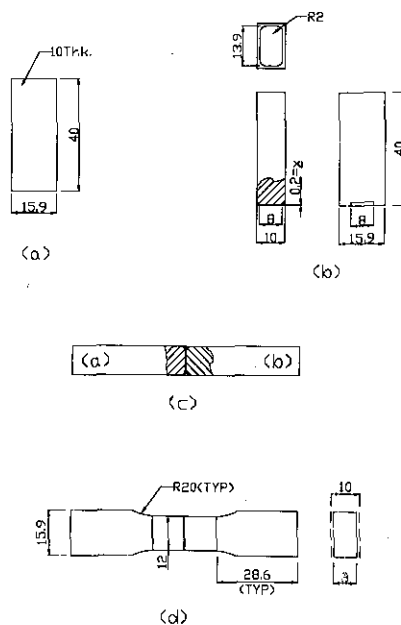

Figure 11. Test sample for solderability test (all dimensions are in mm).

Pull Test

Five test samples were subjected to a pull test for measurement of ultimate tensile strength (UTS). A Universal Testing Machine was used. A successful test must not reveal the separation of nickel coating from the substrate and have UTS forces of around 3,500 Newtons. The UTS values of test coupons examined were in the range of 3,650 to 3,800 Newtons.

MEASUREMENT OF OPTICAL PROPERTIES

A passive thermal control system utilizes the optical properties of its components. In absence of atmosphere, radiation is the only predominant mode of heat exchange in a space environment. The equilibrium temperature of a spacecraft and its subsystems is controlled by the ratio of solar absorptance to infrared emittance. The measurement of both these properties has to be carried out accurately to predict and maintain the temperature of a subsystem in space within the specified limits. The solar absorptance and infrared emittance of all the electroless nickel-plated specimens were measured using a solar reflectometer and emissometer. Both of these instruments provide an average value of solar absorptance and infrared emittance over the entire solar or infrared region.

The solar absorptance and infrared

emittance values of electroless nickel samples were in the range of 0.37 to 0.38 and 0.10 to 0.12, respectively. To evaluate the environmental stability of the coating, the measurements of optical properties were carried out before and after each environmental test—humidity, thermal stability, thermal cycling, and thermovacuum performance test. No change in optical properties of the coating was observed, which indicates their excellent environmental stability in severe space conditions.

EVALUATION OF WEIGHT LOSS

Some of the materials/coatings outgas in the space environment. The outgassing matter may escape, forming a cloud of charged molecules in the vicinity of the spacecraft, or may recondense on the surfaces at low temperatures. Although the weight loss could render a material unsuitable for flight-worthy applications, it is the condensable material that is of much concern because it may result in a drastic change in electrical, thermal, and optical properties of surface; hence, it is imperative to use only those materials and coatings that have low outgassing in the space environment. For a material to be considered for flight usage, the maximum total mass loss and collected volatile condensable material percentage (% TML and % CVCM) are < 1 and < 0.1, respectively.

A standard outgassing test as per ASTM E 595-83 was performed. The test specimen and the boat (container) were conditioned at 23°C and 50% relative humidity for 24 hr. The boat and test specimens were then weighed and placed in the specimen compartment over copper heating bar. A preweighed collector plate was also placed inside the chamber, which was located directly opposite the specimen compartment. The test chamber was then evacuated to a vacuum level of $\geq 10^{-5}$ torr. The temperature of the specimen compartment was raised to 125°C, whereas the collector plate was maintained at 23°C. After 24 hr the test chamber was allowed to cool and attain normal pressure. The specimen and the collector plate were then weighed, and % TML and % CVCM values were obtained.

Because the electroless nickel film is inorganic in nature its outgassing value is very low; absorbed moisture and negligible traces of gas are the only material that can outgas. The % TML and % CVCM values for electroless nickel specimens were only 0.05 and 0.01%, which are well below the specified limits.

CONCLUSIONS

A process of electroless nickel plating on magnesium alloys using the sequence of fluoride activation, electroless nickel deposition, passivation, and heat treatment has been optimized for aerospace applications.

The process provides excellent plating coverage inside narrow holes. The electroless nickel coating so obtained has adequate mechanical properties, corrosion resistance, solderability, and environmental stability for stringent space requirements.
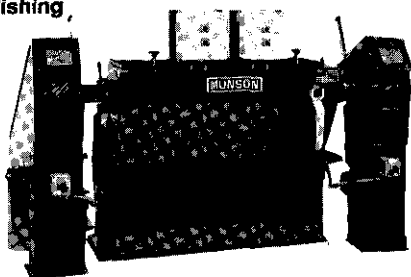
References
1. Sharma, A.K. et al., *Metal Finishing*, 92(3)34; 1993
2. Rajgopal, I. et al., *Metal Finishing*, 88(12):43; 1990
3. Sharma, A.K. et al., *Metal Finishing*, 94(4):16; 1996
4. Kalantary, M.R. et al., *Transactions of the Institute for Metal Finishing*, 71(2): 55; 1993
5. Standard Guide for Autocatalytic Nickel Phosphorus Deposits on Metals for Engineering Use, ASTM 656-91
6. Bayes, M., *Transactions of the Institute for Metal Finishing*, 71(2):62; 1993
7. Sharma, A.K., *Transactions of the Institute of Metal Finishing*, 67:87; 1989
MF